Unidirectional transport of a bead on a single microtubule immobilized in a submicrometre channel

2006 Nanotechnology 17 289

(http://iopscience.iop.org/0957-4484/17/1/049)

INSTITUTE OF PHYSICS PUBLISHING NANOTECHNOLOGY
Nanotechnology **17** (2006) 289–294 doi:10.1088/0957-4484/17/1/049

Unidirectional transport of a bead on a single microtubule immobilized in a submicrometre channel

Ryuji Yokokawa[1], **Yumi Yoshida**[2], **Shoji Takeuchi**[2], **Takahide Kon**[3] **and Hiroyuki Fujita**[2]

[1] Department of Micro System Technology, Ritsumeikan University, 1-1-1, Noji-Higashi, Kusatsu, Shiga 525-8577, Japan
[2] Center for International Research on MicroMechatronics, Institute of Industrial Science, The University of Tokyo, 4-6-1, Komaba, Meguro-ku, Tokyo 153-8505, Japan
[3] Graduate School of Arts and Sciences, The University of Tokyo, 3-8-1, Komaba, Meguro-ku, Tokyo 153-8902, Japan

E-mail: ryuji@se.ritsumei.ac.jp

Received 30 August 2005
Published 5 December 2005
Online at stacks.iop.org/Nano/17/289

Abstract
Artificial nano-scale transportation is demonstrated by reconstructing the intracellular transport in a living cell. The transport system is established on two novel techniques: one is the introduction of a single microtubule filament with controlled polarity in a microfabricated submicrometre channel; the other is the immobilization technique of microtubules by a mercury lamp. To transport a kinesin-coated bead in a designated direction, each microtubule filament is polarly oriented by *in vitro* gliding assay, in which microtubules are carried by the movement of kinesin immobilized on the channel surface. Then, microtubules are immobilized by exposing kinesin to the mercury lamp, which inactivates kinesin but not microtubules. A kinesin-coated bead is newly introduced and carried on the microtubule from one end of the channel to the other as designed. This is an essential component to build up an integrated nano-scale transport system driven by motor proteins.

(Some figures in this article are in colour only in the electronic version)

M This article features online multimedia enhancements

1. Introduction

Analysis and synthesis of an extremely small number of molecules have been much demanded in combinatorial chemistry, high-throughput screening, and detection of an environmental pollutant [1–4]. Recently, assay systems have been downsized to the micrometre scale, and integrated to so-called micro total analysis systems (μTAS) depending on microelectromechanical systems (MEMS). The development has yielded several advantages: the reduction of sample and chemical volume, rapid reactions and price reduction of a device [5–7]. In addition, when the channel size reaches the nanometre size, we are able to focus on a limited amount of liquid and a countable number of molecules: only 600 molecules are present in one femtolitre (10^{-15} l), which corresponds to a cubic micrometre, at a concentration of 1 μM. Researchers have great interest in molecular behaviours in submicrometre channels [8, 9].

However, there are challenging issues to build a nano-fluidic device: manipulating liquid in a nano-channel can hardly be realized by applying pressure using a syringe pump due to the large fluidic resistance. Another issue is the molecular adsorption to the channel wall, which decreases the concentration and may deteriorate the assay [10]. Therefore, there are reports about fabrication techniques for nano-channels much more than their actual use [8, 11–14].

Though the molecular transport by artificial liquid manipulation has limitations in miniaturization in a microfluidic device, nano-scale transport is well performed in a living body [15, 16]. In axon and animal cell bodies, vesicles and organelles of several tens of nanometres in size are carried to a destination where they are required. Such a transportation mechanism is composed of three elements: the energy source of ATP; kinesin, a motor protein which generates force by hydrolysing ATP; and microtubules, which determine the transport path and direction [17–19]. The polarity of microtubules is well oriented in a living cell with the minus end towards the centre and the plus end towards the periphery by their polymerization from centrosome to periphery. The microtubule network produces the unidirectional conveyance of target molecules in the cells by kinesin, since the conventional kinesin moves to the plus end of microtubules [20]. Therefore, imitating the intravital nano-transport system is an approach to transport target molecules in a nano-channel [21–29].

To realize the artificial molecular transport, we have devised a novel reconstruction method of the kinesin–microtubule system integrated with a microfabricated structure. A single filament of microtubule was polarly oriented and immobilized in a submicrometre channel, which was fabricated by micromachining techniques. The kinesin-coated bead was carried on the immobilized microtubule to the designated direction. The reconstructed transport system driven by kinesin and the microtubule can serve as the basic actuator for the nano-scale transport.

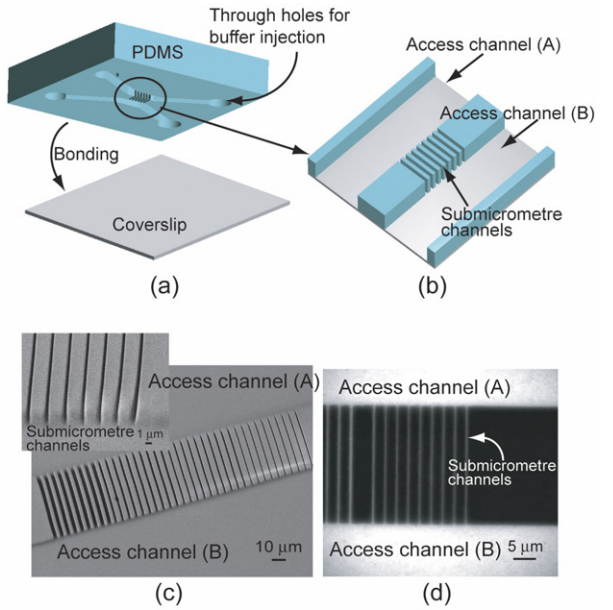

Figure 1. Device configurations. (a) A PDMS replica with grooves is bonded with a coverslip. Samples confined in channels are observed from the bottom of the coverslip by an inverted fluorescent microscope. (b) Submicrometre channels ($L = 50$ μm, $W = 500$–2000 nm, $H = 4$ μm) at the centre part of (a) with access channels ($L = 10$ mm, $W = 300$ μm, $H = 4$ μm). (c) SEM images of channels on a PDMS film. (d) Sealed submicrometre channels filled with a fluorescent dye (tetramethyl rhodamine) are visualized by the fluorescent microscope.

2. Materials and methods

2.1. Submicrometre channel fabrication

Channels were fabricated on a PDMS membrane by a molding technique. PDMS is a well known material to replicate structures down to several tens of nanometres fabricated on a substrate such as a silicon wafer. The transferred channels on the PDMS replica were sealed with a glass coverslip. The overall configuration of channels is shown in figure 1. Parallel channels, ranging from 500 nm to 2 μm in width, connect a pair of micro-scale access channels. Access channels were necessary to inject liquids to submicrometre channels by pipette manipulation.

Two different mask layers were patterned for the mother mould fabrication on a silicon wafer. As the first layer, a negative electron beam (EB) resist (Microposit SAL601-SR7, Shipley) for submicrometre channels was spin-coated on a silicon wafer (30 s at 4000 rpm), and exposed (15 μC cm^{-2}, 20 keV) by an EB-patterning SEM (Tokyo Technology). The resulting structures have nano-scale width after development (MF-312, Shipley). Secondly, UV resist (Microposit S1805, Shipley) was spin-coated on the patterned area (30 s at 4000 rpm), and access micro-scale channels were defined. The second mask layer should be thin enough to visualize the patterned lines for the alignment in UV lithography. Thicknesses of EB and UV resists are around 0.7 and 0.5 μm, respectively. DRIE (Multiplex-ICPRIE, STS) was utilized to etch the wafer by modifying a conventional process condition. The etched depth, which defined the channel depth, was about 4 μm. Resist masks were removed by exposing to oxygen plasma for 5 min using RIE (FA-1, Samco), and the silicon surface was coated by CHF_3 plasma (75 W, 20 ml min^{-1}, 5 min) for the release of a cured PDMS replica.

Replicating channels on PDMS is the next process for the channel fabrication. The PDMS prepolymer (Sylgard184: Curing agent = 10:1, Dow Corning), which contains a reagent (DK Q8-8011, Dow Corning) to make PDMS hydrophilic, was poured on the master and cured for 1 h at 90 °C. Submicrometre channels (length = 50 μm, width = 500–2000 nm, height = 4 μm) and access channels (length = 10 mm, width = 300 μm, height = 4 μm) were transferred to the PDMS surface as shown in figure 1(c). When the channel size decreases to the range of submicrometres, it becomes drastically difficult to inject liquids. To solve the problem, our PDMS was modified to be less hydrophobic by adding the reagent to PDMS prepolymer. The PDMS replica was adhered to a glass coverslip to seal the channels, and they were examined by injecting a fluorescent dye (5-(and-6)-carboxytetramethylrhodamine, Molecular Probe, C-1171) as shown in figure 1(d). Owing to the treatment, submicrometre channels were easily filled with the dye. This proves that there is no leakage observed at the interface between PDMS and the coverslip.

2.2. Protein preparation and observation

A kinesin heavy chain (110 kDa) derived from *Drosophila melanogaster* with a GST tag (26 kDa) was expressed in *E. coli*. Purification was performed using GST-kinesin affinities with

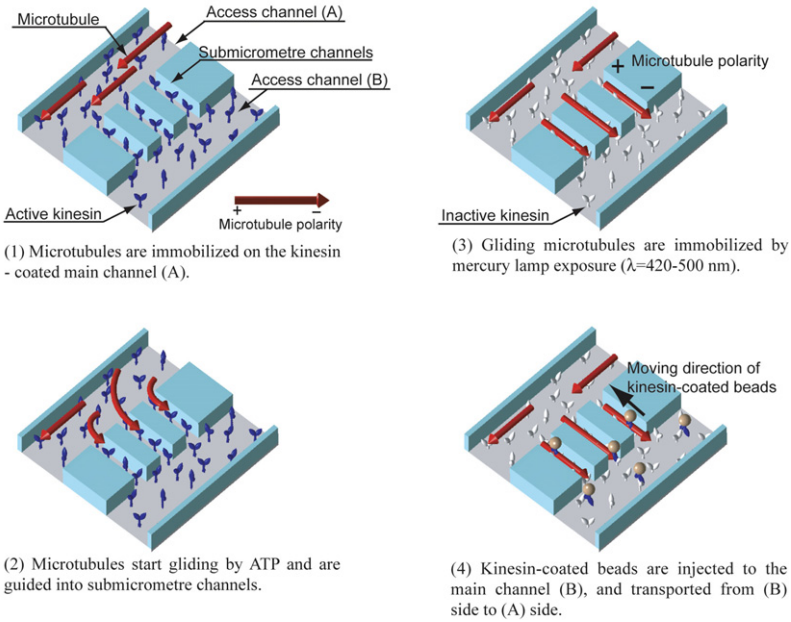

Figure 2. Process flow of the assay. It realizes the unidirectional transportation of beads (diameter = 320 nm) on a single microtubule filament immobilized in a submicrometre channel. (1) Microtubules are immobilized on the kinesin-coated main channel (A). (2) Microtubules start gliding by ATP and are guided into submicrometre channels. (3) Gliding microtubules are immobilized by mercury lamp exposure (λ = 420–500 nm). (4) Kinesin-coated beads are injected into the main channel (B), and transported from the (B) side to the (A) side.

glutathione-Sepharose (17-5132-01, Amersham Biosciences) and microtubules. The final concentration of kinesin was about 40 μg ml^{-1} in 25 mM Tris acetate, 200 mM K acetate, 10 mM $MgSO_4$, 10 mM ATP and 1 mM EGTA, and stored in liquid nitrogen. Kinesin-coated beads were prepared by mixing purified kinesin and carboxylate-modified beads (diameter = 320 nm, PC00N/3079, BangsLab).

Tubulin, the monomer of microtubules, was prepared from four porcine brains by two cycles of temperature-dependent polymerizations and phosphocellulose chromatography [30, 31]. Tubulin was stored in liquid nitrogen at the concentration of 4 mg ml^{-1} in 0.5 mM guanosine 5′-triphosphate sodium salt hydrate (GTP) in PC buffer (100 mM PIPES-NaOH (pH 6.8), 1 mM EGTA, 1 mM $MgSO_4$). The purified tubulin was labelled with 5-(and-6)-carboxytetramethylrhodamine and stored at the concentration of 4 mg ml^{-1}. The preparation protocol described in the references was modified for the small amount of tubulin [31, 32].

Non-fluorescent microtubules were polymerized at 37 °C in PC buffer containing 1 mM $MgSO_4$ and 1 mM GTP, and examined by a dark-field microscope (BX50, UPLFLN 40X, Olympus) equipped with a charge-coupled device (CCD) camera (CCD-300-RC, Dage-MTI), an image intensifier unit (C9016-01, Hamamatsu), a video enhancement system (XL-20, Olympus), and a digital video-cassette recorder (DSR-11, Sony). Fluorescent microtubules were polymerized at the ratio of 1:10 for labelled and non-fluorescent tubulin, which were also examined before the experiments by the dark-field and fluorescent microscopes (IX71, UPLFLN 100XOI, Olympus). A general assay buffer for the non-fluorescent observation was BRB80 (80 mM PIPES-NaOH (pH 6.8), 1 mM $MgCl_2$, 1 mM EGTA). Another buffer for the fluorescent observation was BRB80 supplemented with an oxygen-scavenger system (36 μg ml^{-1} catalase, 4.5 mg ml^{-1} glucose, 216 μg ml^{-1} glucose oxidase, 1% β-mercaptoethanol), which prevents microtubule depolymerization by excited oxygen species. We achieved low intensity of illumination and fluorescence, which also inhibit the generation of excited oxygen species in a buffer, by the combination of two pieces of equipment: ND filters (ND50, 25, 6) to weaken the illumination by a mercury lamp, and an image intensifier unit to detect the weak fluorescence of the microtubules.

3. Results and discussion

3.1. Microtubule introduction to a submicrometre channel

Figure 2 illustrates the experimental procedure to orient and immobilize a microtubule in each channel, and to transport kinesin-coated beads on it. Kinesin introduction to the submicrometre channels was as easy as the fluorescent dye case shown in figure 1(d). Not only the glass surface but the PDMS wall was coated with kinesin. Excess kinesin was washed out by BRB80 buffer solution, and microtubules were injected into the access channel (A). They were trapped by kinesin on the channel surface, but did not enter the submicrometre channels, because the buffer flow was only applied to the access channel (A) with the other channel (B) closed. Unbound microtubules in the channel (A) were removed by buffer flushing, which allows us to have trapped microtubules as illustrated in figure 2(1).

ATP injection causes the gliding assay of microtubules and some of them glide into submicrometre channels as shown in figure 2(2) (video file 1: available at stacks.iop.org/Nano/17/289). The number of microtubules in each channel depends on the concentration of microtubules,

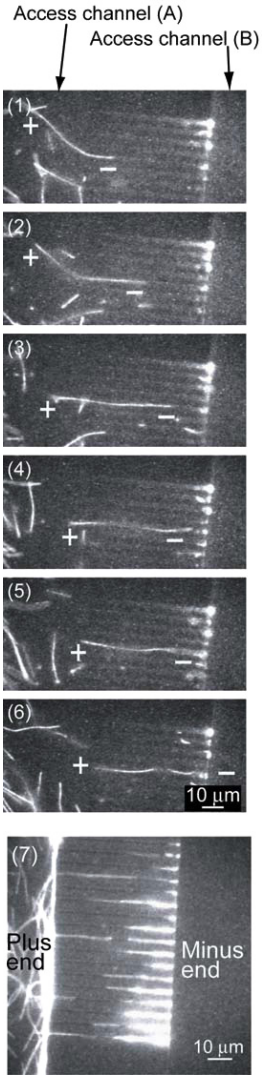

Figure 3. Fluorescent microtubule guidance into submicrometre channels. (1)–(6) Sequential pictures (15 s interval) of a microtubule (690 nm s^{-1}) gliding into a channel (750 nm in width). (7) Microtubules are introduced in multiple channels.

size of channels, and assay time. The number of microtubules introduced in a channel increases with the increase of these parameters. We have successfully introduced a fluorescent microtubule in each channel by optimizing parameters as follows: 40 μg ml^{-1} for microtubule concentration, 500–750 nm for channel width, and 10 min for assay time. Sequential images with 15 s intervals are shown in figure 3. Once the movement of the microtubule head was confined at the entrance of a submicrometre channel, it kept gliding into the channel without making a U-turn. This is caused by the stiff structure of microtubules compared with other filaments such as actin and DNA. A few blurred parts of the microtubule in figures 3(4)–(6) were caused by vertical gliding movement of kinesin on PDMS walls. As a result, the leading head of the microtubule had reached the exit of the channel.

Though the technique provides the perfect orientation of microtubules, there are some limitations in their positioning. Precise allocation as designated in the channel is not

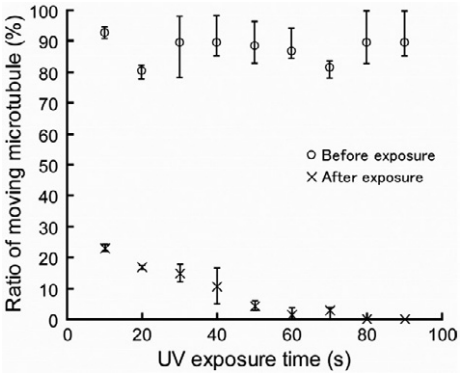

Figure 4. Ratio of moving microtubules before and after exposure. The ratio was determined by counting the number of microtubules. About 90% of microtubules were gliding on a glass surface, but the ratios drastically drop after lamp exposure. The wavelength of $\lambda = 420$–500 nm was optimized using several filters.

necessarily achieved due to variances in microtubule length and timing of microtubules entering channels. When the assay time is too long, microtubules may glide through the channels.

Each kinesin immobilized on the glass surface tries to move to the plus end of the microtubule; i.e. the leading head of the microtubule is the minus end in the gliding assay. Therefore, the polarity of the microtubule is oriented in the submicrometre channels as indicated by + and − in figures 2(3) and 3.

3.2. Microtubule immobilization

The next significant step is to immobilize the microtubule in the submicrometre channels as shown in figure 2(3). We have established an immobilization technique of non-fluorescent microtubules by exposing kinesin to a mercury UV lamp at the optimized wavelength of 420–500 nm. The exposure condition was optimized by combining four filters (IF550, Y50, L42, Robon). Even after kinesin molecules are inactivated by the exposure, they keep holding microtubules. The microtubules also keep their function to guide kinesin to the plus end. The technique enables the immobilization of the polarly oriented microtubule in the channel without any complicated techniques, so that the polarity of each microtubule can be perfectly determined as observed in a living cell.

The exposure time of the mercury lamp was optimized based on the relationship between microtubule activity and exposure time as shown in figure 4. The lamp was switched on during the gliding assay, and the ratio of moving microtubules was measured before and after the exposure. The duration of exposure was varied from 10 to 90 s. About 90% of the microtubules were moving before the exposure, and the ratio drastically drops even after a short time exposure. It takes 60 s to immobilize all microtubules. The technique will also be applicable to other motor proteins such as dynein, myosin, and F_1 ATPase.

3.3. Bead transport on the immobilized microtubule

In order to examine the microtubule, bead assay was performed in the channel as illustrated in figure 2(4). Beads were

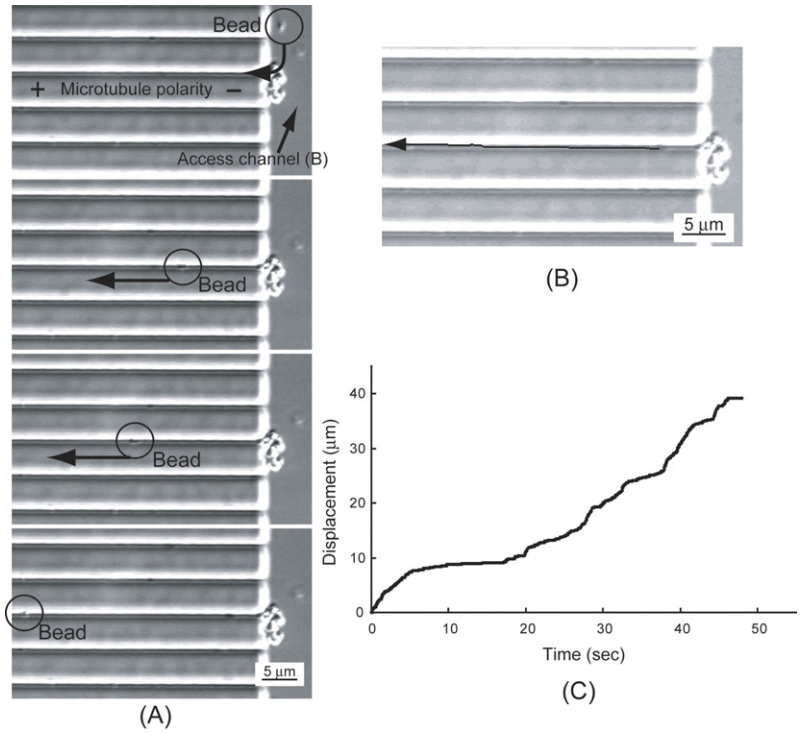

Figure 5. Unidirectional transportation of a bead in a channel. (A) Sequential pictures (20 s interval) of a kinesin-coated bead (747 nm s^{-1}, bead diameter = 320 nm) transported on a microtubule (not visualized) immobilized in a submicrometre channel of 500 nm in width. (B) The tracked path of the bead. (C) The time course of the total displacement of the bead.

coated with active kinesin prior to the assay, and injected into the access channel (B), because the minus end of the microtubule is supposed to face the channel (B). Kinesin-coated beads were transported on the immobilized microtubule in a 500 nm width channel, and the focused bead was transported toward the plus end (access channel (A)) on the microtubule as shown in figure 5(A) (video file 2: available at stacks.iop.org/Nano/17/289). This proves that the microtubule was oriented and immobilized as designed. The result also supports the conclusion that the lamp exposure inactivates kinesin coated on the channel surface, but the immobilized microtubule remains active to serve as a rail molecule for the bead transportation.

The transported bead was tracked by software (Move-tr/2D and Cosmos32, Library) to examine its moving direction and velocity. The red line in figure 5(B) indicates the trace of the bead, in which the moving direction is from right to left as shown in the sequential pictures in figure 5(A). The time course of the total displacement is plotted in figure 5(C), and the average bead velocity was determined as 747 nm s^{-1} by the graph gradient. The result proves that the bead was transported by the kinesin movement on the microtubule for the following two reasons. The bead velocity is comparable to the one in the conventional bead assay in a flow cell. The kinesin-driven beads have much lower velocity than that of flowing beads (21 μm s^{-1}) driven by the pressure difference between the inlet and outlet of the channel.

4. Conclusion

This is the first achievement of a transportation system using a single microtubule filament immobilized in an artificial structure. The system consists of two different components: actuators of motor proteins and micromachined structures, which are prepared by the bottom-up and top-down technology, respectively. A bottom-up technique, bioengineering, is not able to produce millimetre scale devices, but is able to produce bio-actuators up to several tens of nanometres in large quantity. On the other hand, the minimum size of actuators fabricated by one of the top-down technologies, micromachining, is limited to the range of sub-micrometres. Compensating drawbacks with each other, two technologies are successfully integrated to realize a biomimetic nano-scale transportation system.

Our approach focused on processing a single microtubule and we achieved perfect control of its orientation. This is the distinctive difference from conventional attempts to utilize numbers of oriented microtubules for carrying objects unidirectionally in a millimetre-scale flow cell [33–35]. The orientation process has a stochastic nature; thus, some misorientation is inevitable [21]. Since our transport system has each microtubule filament oriented in a channel, the transport direction is absolutely defined.

The established technique will be an important element in a more complex system which consists of multiple microtubules fixed in channels for two-dimensional transportation. Microtubules can be manipulated without any additional force being applied from outside such as the optical force by optical tweezers. Just by fabricating submicrometre channels on a PDMS membrane, we allocate microtubules for the transportation of objects. For example, when two microtubules are designed crossing each other, two kinesin-coated beads will be transported on each microtubule and collide at the intersection. When each bead carries

different molecules on the surface, they may react at the collision. This must be the smallest artificial chemical reaction system, implying a nano-scale lab-on-a-chip. Therefore, this is a fundamental result to reconstruct the intracellular transportation system in a microfabricated device.

Acknowledgments

The authors would like to thank Dr Masaya Nishiura and Mr Toshifumi Mogami from the University of Tokyo for helping with the tubulin preparation. This research was partially supported byThe Ministry of Education, Culture, Sports, Science and Technology, Japan, Grant-in-Aid for Scientific Research (B), 17310082, 2005. One of the authors, RY, is supported by the Grant-in-Aid for JSPS Fellows, The Ministry of Education, Culture, Sports, Science and Technology, Japan.

References

[1] Maxwell I E 1998 Combinatorial chemistry: connecting with catalysis *Nature* **394** 325–6
[2] Lehn J M and Eliseev A V 2001 Dynamic combinatorial chemistry *Science* **291** 2331–2
[3] Smith A 2002 Screening for drug discovery: the leading question *Nature* **418** 453–9
[4] Yea K H, Lee S, Kyong J B, Choo J, Lee E K, Joo S W and Lee S 2005 Ultra-sensitive trace analysis of cyanide water pollutant in a PDMS microfluidic channel using surface-enhanced Raman spectroscopy *Analyst* **130** 1009–11
[5] Reyes D, Iossifidis D, Auroux P and Manz A 2002 Micro total analysis systems. 1. introduction, theory, and technology *Anal. Chem.* **74** 2623
[6] Auroux P, Iossifidis D, Reyes D R and Manz A 2002 Micro total analysis systems. 2. Analytical standard operations and applications *Anal. Chem.* **74** 2637–52
[7] Manz A, Graber N and Widmer H M 1990 Miniaturized total chemical analysis systems: a novel concept for chemical sensing *Sensors Actuators* B **1** 244–8
[8] Sivanesan P, Okamoto K, English D, Lee C S and Devoe D L 2005 Polymer nanochannels fabricated by thermomechanical deformation for single-molecule analysis *Anal. Chem.* **77** 2252–8
[9] Mijatovic D, Eijkel J C T and Berg A v d 2005 Technologies for nanofluidic systems: top-down vs. bottom-up—a review *Lab Chip* **5** 492–500
[10] Drazer G, Koplik J, Acrivos A and Khusid B 2002 Adsorption phenomena in the transport of a colloidal particle through a nanochannel containing a partially wetting fluid *Phys. Rev. Lett.* **89** 244501
[11] Lee C, Yang E-H, Myung N V and George T 2003 A nanochannel fabrication technique without nanolithography *Nano Lett.* **3** 1339–40
[12] Hibara A, Saito T, Kim H, Tokeshi M, Ooi T, Nakao M and Kitamori T 2002 Nanochannels on a fused-silica microchip and liquid properties investigation by time-resolved fluorescence measurements *Anal. Chem.* **74** 6170–6
[13] Haneveld J, Jansen H, Berenschot E, Tas N and Elwenspoek M 2003 Wet anisotropic etching for fluidic 1D nanochannels *J. Micromech. Microeng.* **13** S62–6
[14] Stern M B, Geis M W and Curtin J E 1997 Nanochannel fabrication for chemical sensors *J. Vac. Sci. Technol.* B **15** 2887–91
[15] Vale R D, Reese T S and Sheetz M P 1985 Identification of a novel force-generating protein, kinesin, involved in microtubule-based motility *Cell* **42** 39–50
[16] Alberts B, Johnson A, Lewis J, Raff M, Roberts K and Walter P 2002 *Molecular Biology of the Cell* 4th edn (NY, USA: Garland Publishers) ISBN 0815340729
[17] Howard J, Hudspeth A J and Vale R 1989 Movement of microtubules by single kinesin molecules *Nature* **342** 154–9
[18] Svoboda K, Schmidt C, Schnapp B and Block S 1993 Direct observation of kinesin stepping by optical trapping interferometry *Nature* **365** 721–7
[19] Vale R D and Milligan R A 2000 The way things move: looking under the hood of molecular motor proteins *Science* **288** 88–95
[20] Vale R D 2003 The molecular motor toolbox for intracellular transport *Cell* **112** 467–80
[21] Yokokawa R, Takeuchi S, Kon T, Nishiura M, Sutoh K and Fujita H 2004 Unidirectional transport of kinesin-coated beads on microtubules oriented in a microfluidic device *Nano Lett.* **4** 2265–70
[22] Clemmens J, Hess H, Doot R, Matzke C M, Bachand G D and Vogel V 2004 Motor-protein 'roundabouts': microtubules moving on kinesin-coated tracks through engineered network *Lab Chip* **4** 83–6
[23] Jia L and Hancock W 2004 Microscale transport and sorting by kinesin molecular motors *Biomed. Microdev.* **6** 67–74
[24] Bachand G D, Rivera S B, Boal A K, Gaudioso J, Liu J and Bunker B C 2004 Assembly and transport of nanocrystal cdse quantum dot nanocomposites using microtubules and kinesin motor proteins *Nano Lett.* **4** 817–21
[25] Moorjani S, Jackson T and Hancock W 2003 Lithographically patterned channels spatially segregate kinesin motor activity and effectively guide microtubule movements *Nano Lett.* **3** 633–7
[26] Brown T B and Hancock W O 2002 A polarized microtubule array for kinesin-powered nanoscale assembly and force generation *Nano Lett.* **2** 1131–5
[27] Limberis L, Magda J J and Stewart R J 2001 Polarized alignment and surface immobilization of microtubules for kinesin-powered nanodevices *Nano Lett.* **1** 277–80
[28] Hiratsuka Y, Tada T, Oiwa K, Kanayama T and Uyeda T Q 2001 Controlling the direction of kinesin-driven microtubule movements along microlithographic tracks *Biophys. J.* **81** 1555–61
[29] Yokokawa R, Takeuchi S, Kon T, Nishiura M, Ohkura R, Edamatsu M, Sutoh K and Fujita H 2004 Hybrid nanotransport system by biomolecular linear motors *IEEE/ASME J. Microelectromech. Syst.* **13** 612–9
[30] Mitchison T J and Kirschner M W 1984 Microtubule assembly by isolated centrosomes; dynamic instability of microtubule growth *Nature* **312** 232–42
[31] Hyman A, Drechsel D, Kellogg D, Salser S, Sawin K, Steffen P, Wordeman L and Mitchison T 1991 Preparation of modified tubulins *Methods Enzymol.* **196** 478–85
[32] Mitchison T J 1989 Polewards microtubule flux in the mitotic spindle: evidence from photoactivation of fluorescence *J. Cell Biol.* **109** 637–52
[33] Bohm K, Stracke R, Muhlig P and Unger E 2001 Motor protein-driven unidirectional transport of micrometer-sized cargoes across isopolar microtubule arrays *Nanotechnology* **12** 238–44
[34] Prots I, Stracke R, Unger E and Bohm K 2003 Isopolar microtubule arrays as a tool to determine motor protein directionality *Cell Biol. Int.* **27** 251–3
[35] Stracke R, Bohm K J, Burgold J, Schacht H and Unger E 2000 Physical and technical parameters determining the functioning of a kinesin-based cell-free motor system *Nanotechnology* **11** 52–6